

Washington University School of Medicine

Digital Commons@Becker

Open Access Publications

2020

Human recombinant apyrase therapy protects against myocardial ischemia/reperfusion injury and preserves left ventricular systolic function in rats, as evaluated by 7T cardiovascular magnetic resonance imaging

Ziqian Xu
Sichuan University

Wei Chen
Kunming Medical College

Ruzhi Zhang
Sichuan University

Lei Wang
Sichuan University

Ridong Chen
APT Therapeutics Inc.

See next page for additional authors
Follow this and additional works at: https://digitalcommons.wustl.edu/open_access_pubs

Please let us know how this document benefits you.

Recommended Citation

Xu, Ziqian; Chen, Wei; Zhang, Ruzhi; Wang, Lei; Chen, Ridong; Zheng, Jie; and Gao, Fabao, "Human recombinant apyrase therapy protects against myocardial ischemia/reperfusion injury and preserves left ventricular systolic function in rats, as evaluated by 7T cardiovascular magnetic resonance imaging." *Korean Journal of Radiology*. 21, 6. 647 - 659. (2020).
https://digitalcommons.wustl.edu/open_access_pubs/9403

This Open Access Publication is brought to you for free and open access by Digital Commons@Becker. It has been accepted for inclusion in Open Access Publications by an authorized administrator of Digital Commons@Becker. For more information, please contact vanam@wustl.edu.

Authors

Ziqian Xu, Wei Chen, Ruzhi Zhang, Lei Wang, Ridong Chen, Jie Zheng, and Fabao Gao



Human Recombinant Apyrase Therapy Protects Against Myocardial Ischemia/Reperfusion Injury and Preserves Left Ventricular Systolic Function in Rats, as Evaluated by 7T Cardiovascular Magnetic Resonance Imaging

Ziqian Xu, PhD¹, Wei Chen, PhD², Ruzhi Zhang, MD¹, Lei Wang, BD¹, Ridong Chen, PhD³, Jie Zheng, PhD⁴, Fabao Gao, MD, PhD¹

¹Department of Radiology, West China Hospital, Sichuan University, Chengdu, China; ²Department of Radiology, The First Affiliated Hospital of Kunming Medical College, Kunming, China; ³APT Therapeutics Inc., St Louis, MO, USA; ⁴Mallinckrodt Institute of Radiology, Washington University School of Medicine, St. Louis, MO, USA

Objective: The occurrence of intramyocardial hemorrhage (IMH) and microvascular obstruction (MVO) in myocardial infarction (MI), known as severe ischemia/reperfusion injury (IRI), has been associated with adverse remodeling. APT102, a soluble human recombinant ecto-nucleoside triphosphate diphosphohydrolase-1, can hydrolyze extracellular nucleotides to attenuate their prothrombotic and proinflammatory effects. The purpose of this study was to temporally evaluate the therapeutic effect of APT102 on IRI in rats and to elucidate the evolution of IRI in the acute stage using cardiovascular magnetic resonance imaging (CMRI).

Materials and Methods: Fifty-four rats with MI, induced by ligation of the origin of the left anterior descending coronary artery for 60 minutes, were randomly divided into the APT102 ($n = 27$) or control ($n = 27$) group. Intravenous infusion of APT102 (0.3 mg/kg) or placebo was administered 15 minutes before reperfusion, and then 24 hours, 48 hours, 72 hours, and on day 4 after reperfusion. CMRI was performed at 24 hours, 48 hours, 72 hours, and on day 5 post-reperfusion using a 7T system and the hearts were collected for histopathological examination. Cardiac function was quantified using cine imaging and IMH/edema using T2 mapping, and infarct/MVO using late gadolinium enhancement.

Results: The extent of infarction ($p < 0.001$), edema ($p < 0.001$), IMH ($p = 0.013$), and MVO ($p = 0.049$) was less severe in the APT102 group than in the control group. IMH size at 48 hours was significantly greater than that at 24 hours, 72 hours, and 5 days after reperfusion (all $p < 0.001$). The left ventricular ejection fraction (LVEF) was significantly greater in the APT102 group than in the control group ($p = 0.006$). There was a negative correlation between LVEF and IMH ($r = -0.294$, $p = 0.010$) and a positive correlation between IMH and MVO ($r = 0.392$, $p < 0.001$).

Conclusion: APT102 can significantly alleviate damage to the ischemic myocardium and microvasculature. IMH size peaked at 48 hours post reperfusion and IMH is a downstream consequence of MVO. IMH may be a potential therapeutic target to prevent adverse remodeling in MI.

Keywords: Myocardial ischemia/reperfusion injury; Intramyocardial hemorrhage; Microvascular obstruction; Cardiovascular magnetic resonance; APT102

Received: November 12, 2019 **Revised:** January 9, 2020 **Accepted:** February 5, 2020

This study was supported by the National Natural Science Foundation of China (81930046, 81829003, 81520108014, and 81771800), the State's Key Project of Research and Development Plan of China (2016YFA0201402), and the international cooperation project of science and technology program of Sichuan (2017HH0045).

Corresponding author: Fabao Gao, MD, PhD, Department of Radiology, West China Hospital, Sichuan University, No. 37 Guoxue Road, Chengdu 610041, China.

• Tel: (86) 18980602020 • Fax: (86) 028-85164081 • E-mail: gaofabao@wchscu.cn

This is an Open Access article distributed under the terms of the Creative Commons Attribution Non-Commercial License (<https://creativecommons.org/licenses/by-nc/4.0>) which permits unrestricted non-commercial use, distribution, and reproduction in any medium, provided the original work is properly cited.

INTRODUCTION

In patients with acute ST-segment elevation myocardial infarction (STEMI), timely myocardial reperfusion therapeutic methods can effectively salvage viable cardiomyocytes, limit the extent of myocardial infarction (MI), improve long-term myocardial function, reduce mortality, and prevent heart failure (1). However, the process of myocardial reperfusion can itself concurrently induce additional capillary damage and cardiomyocyte injury, a common phenomenon known as myocardial ischemia/reperfusion injury (IRI) (2), which may cause ventricular arrhythmia (3), myocardial stunning (4), microvascular obstruction (MVO) (5), intramyocardial hemorrhage (IMH) (6), and lethal myocardial reperfusion injury (7). Although the underlying mechanisms of IRI have not been completely elucidated, previous studies have found that MVO and IMH were independent predictors of larger infarct size, lower left ventricular (LV) systolic function, and major adverse cardiac events (8). Hence, early detection and preventive or active treatment of IMH and MVO may significantly influence clinical judgements and outcomes.

The extracellular nucleotides, adenosine triphosphate (ATP) and adenosine diphosphate (ADP), are released from injured cardiomyocytes into the extracellular interstitium where they bind to the purinergic receptors P2X and P2Y on platelets, endothelial cells, and immune cells, which then secrete prothrombotic and proinflammatory cytokines (9). Human ecto-nucleoside triphosphate diphosphohydrolase (E-NTPDase)-1 (CD39) is an extracellular apyrase that hydrolyzes ATP and ADP to adenosine monophosphate (AMP) and attenuates prothrombotic and proinflammatory effects without increasing bleeding risk, while CD39 activity is lost with prolonged IRI (10, 11). Previous studies have demonstrated that the administration of APT102, a soluble human recombinant CD39, can alleviate IRI following ischemic stroke (12), lung infarction (13), lung isografts (14), and MI (15). Therefore, the purpose of this study was to temporally evaluate the therapeutic effects of human recombinant apyrase APT102 on IRI in rats and to elucidate the evolution of IRI in the acute stage using cardiovascular magnetic resonance imaging (CMRI).

MATERIALS AND METHODS

Animal Preparation

A total of 60 female Sprague-Dawley rats (weight,

250–270 g; age, 9–10 weeks) were subjected to ligation of the origin of the left anterior descending coronary artery for 60 minutes. Six rats died due to arrhythmia during the ischemic period; 54 rats were randomly assigned to either the APT102 ($n = 27$) or control ($n = 27$) group. APT102 (0.3 mg/kg) or an equal concentration of a placebo was injected via the tail vein at 15 minutes before reperfusion, and then at 1, 2, 3, and 4 days afterward. The animal model of myocardial ischemia/reperfusion was established as previously described (16). All experimental procedures were approved by the experimental Animal Ethics Committee of West China Hospital, Sichuan University (Chengdu, China).

CMRI Protocols

CMRI was performed using a small animal 7T magnetic resonance imaging system (BioSpec 70/30; Bruker, Karlsruhe, Germany) equipped with a 4-channel rat heart surface coil. Rats were imaged on days 1, 2, 3, and 5 after reperfusion. The pre-scanning preparation was conducted as previously described (16). Gadopentetate dimeglumine (Gd-DTPA, 0.15 mmol/kg; SA Instruments, Inc., Stony Brook, NY, USA) was injected through the tail vein and late gadolinium enhancement (LGE) imaging was performed 10 minutes after injection.

Images of the heart were obtained using a gradient-echo sequence. Gated multi-slice IntraGate Fast Low Angle Shot-cine was then performed to confirm the heart position in three planes (short-axis, and 2- and 4-chamber long axis) to determine the location of the LV using the following scanning parameters: repetition time/echo time (TR/TE) = 8 ms/3 ms, matrix (MTX) = 256 × 256, field of view (FOV) = 5 × 5 cm, and slice thickness = 1.5 mm. T2 mapping was acquired using a fast spin echo technique from the cardiac base to apex (scanning parameters: TR/TE = 1500 ms/10, 20, and 30 ms, flip angle = 180°, acquisition MTX = 192 × 192, FOV = 5 × 5 cm, number of slices = 6 or 7, slice thickness = 1.5 mm, and slice gap = 1.5 mm). LGE was acquired using a fast imaging with steady precession (FISP) technique (scanning parameters: TR/TE = 5.2 ms/1.8 ms, flip angle = 25°, no inversion recovery pulse, MTX = 256 × 256, FOV = 5 × 5 cm, slice thickness = 1.5 mm, slice gap = 1.5 mm).

Histopathology

Rats were sacrificed at 24 hours ($n = 5$ for each group), 48 hours ($n = 5$ for each), 72 hours ($n = 5$ for each), or on day 5 ($n = 12$ for each) after reperfusion. Hearts were

explanted and fixed with 4% paraformaldehyde solution at 4°C for 48 hours. According to the scanning slices, the hearts were sectioned into consecutive 1.5-mm-thick slices along the short-axis plane. Each slice was photographed using a digital camera (D7500; Nikon Corporation, Tokyo, Japan) to register and quantify IMH. Hematoxylin and eosin (H&E) staining was used to qualitatively assess necrosis, inflammation, IMH, and MVO. Two observers with at least 5 years' experience in pathological examination blinded to the CMR images and groups separately analyzed all gross slides and histopathologic images. Disagreements were resolved by consensus.

Data Analysis

Two radiologists with a minimum of 7 years related experience, blinded to the pathology results and group distributions, analyzed all CMR images and calculated averages. Three T2 images (TE = 10, 20, and 30 ms) were amalgamated using custom software written in MATLAB (version 7.1; MathWorks, Natick, MA, USA). On T2 mapping images, the area of myocardial edema was defined as a mean signal intensity threshold of two standard deviations (SDs) above the mean remote myocardium (17) and IMH was defined as a hypointense core within a hyperintense area (18). Meanwhile, on LGE images, MI was defined and quantified as an area with a mean signal intensity at least 5 SDs above the remote myocardium (19). MVO was defined as the non-contrasted enhancement zone within the infarct region (20). The example analysis of these parameters is shown in Supplementary Figure 1. All parameters were manually measured using ImageJ software (National Institutes of Health, Bethesda, MD, USA). The epicardial and endocardial outlines (papillary muscles were excluded from the endocardium) at left ventricular end-diastole and left ventricular end-systole were manually drawn on cine images, slice by slice. The left ventricular myocardial volume (LVMV), left ventricular end-diastolic volume (LVEDV), left ventricular end-systolic volume (LVESV), stroke volume (SV), and left ventricular ejection fraction (LVEF) were then calculated by multiplying the slice thickness and slice gap. The total volume of MI, edema, IMH, and MVO in cubic centimeters was calculated by multiplying the area by the slice thickness and slice gap and expressed as a percentage of LVMV.

Statistical Analysis

Quantitative data were tested for normal distribution

using the Kolmogorov-Smirnov test. Levene's test was used to assess the homogeneity of variance. Time sequential changes in T2 values and the extent of edema, IMH, MI, and MVO, as well as cardiac function were evaluated using two-way repeated measures analyses of variance with the least significance difference and post hoc Bonferroni's test for multiple comparisons. The Greenhouse-Geisser correction was applied when Mauchley's test indicated that the assumption of sphericity had been violated. The partial correlation between LVEF and the extent of MI, edema, IMH, and MVO was assessed. All statistical analyses were performed using SPSS Statistics version 23.0 (IBM Corp., Armonk, NY, USA). Interobserver and intraobserver agreement was calculated using the intraclass correlation coefficient. Limits of agreement for IMH size between the T2 mapping and the gross pathology images were determined using Bland-Altman analysis performed on Prism (version 7.0; GraphPad, San Diego, CA, USA). Data are expressed as the mean \pm SD or as numbers (percentages). A probability (*p*) value of < 0.05 was considered statistically significant.

RESULTS

One rat in the control group died of respiratory failure during scanning. Scanning images from one rat in the control group and two rats in the APT102 group contained motion artifacts and could not be analyzed and were thus excluded from the analysis. A flow chart is shown in Figure 1.

APT102 Reduced MI Size

The infarct size was significantly smaller in the APT102 group than in the control group ($F = 23.627$, $p < 0.001$) (Table 1). There were significant main effects at all time points ($F = 143.011$, $p < 0.001$) (Table 1), but no significant interactions between groups and time points ($F = 1.017$, $p = 0.361$) (Table 1). Infarct size at 24 hours was significantly greater than at 48 hours, 72 hours, and on day 5 ($p = 0.008$, $p < 0.001$, and $p < 0.001$, respectively) (Table 1, Fig. 2A) after reperfusion. The infarct size was significantly smaller in the APT102 group than in the control group at 24 hours ($18.0 \pm 4.8\%$ vs. $26.7 \pm 5.7\%$, respectively, $p = 0.002$), 48 hours ($17.1 \pm 4.3\%$ vs. $25.7 \pm 6.0\%$, respectively, $p = 0.002$), 72 hours ($11.6 \pm 2.6\%$ vs. $21.5 \pm 6.0\%$, respectively, $p < 0.001$), and on day 5 ($5.8 \pm 1.5\%$ vs. $16.2 \pm 4.0\%$, respectively, $p < 0.001$) after reperfusion, as shown in Figure 2A.

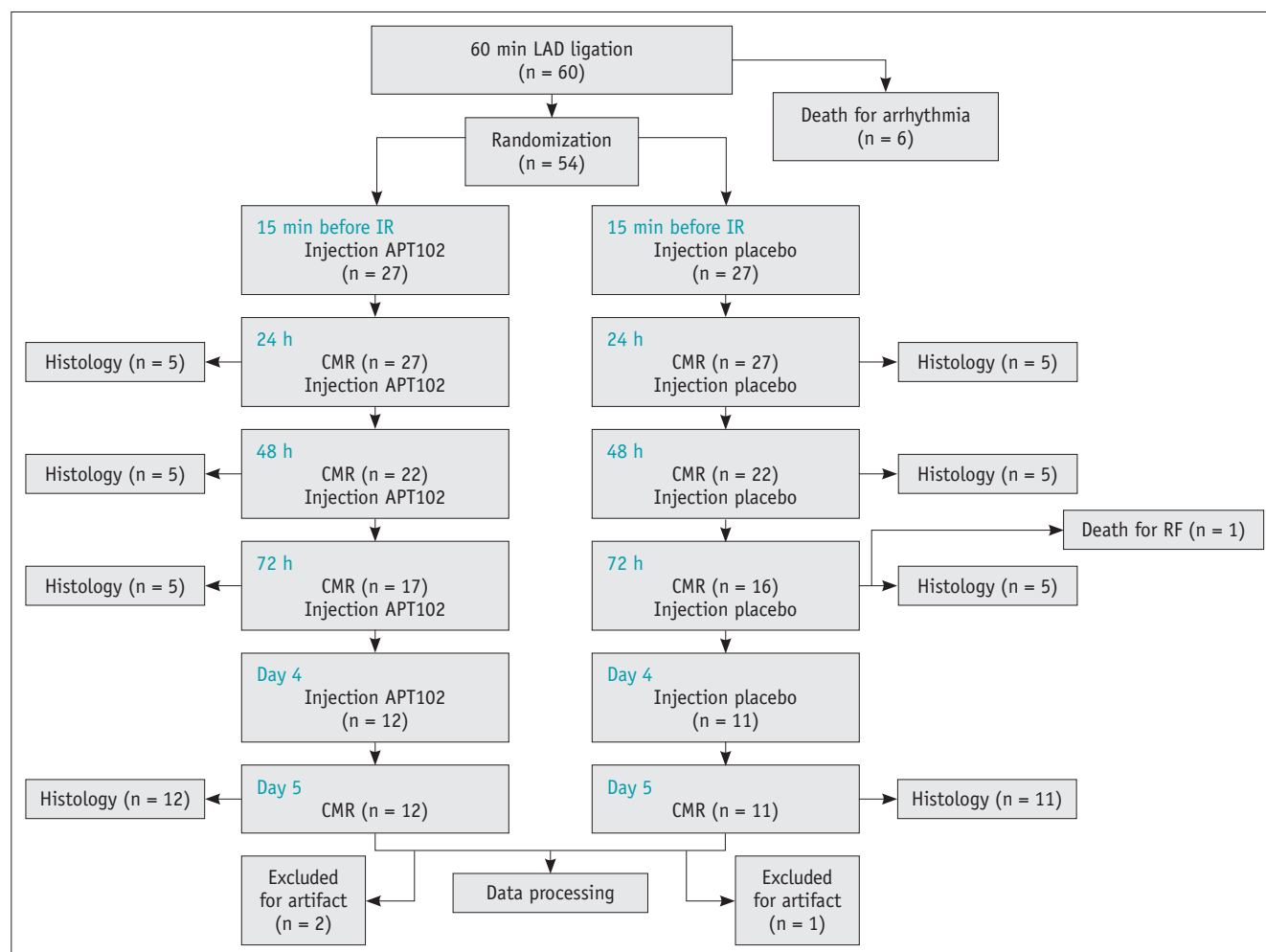


Fig. 1. Flow chart of study protocol. CMR = cardiovascular magnetic resonance, IR = ischemia/reperfusion, LAD = left anterior descending branch, RF = respiratory failure

Table 1. Comparison of Myocardial Characterization according to Time Points and Groups

Variable	24 h	48 h	72 h	Day 5	Group		Time		Group x Time	
					F	P	F	P	F	P
Infarct size (%)										
Control (n = 10)	26.7 ± 5.7	25.7 ± 6.0	21.5 ± 6.0	16.2 ± 4.0	23.627	< 0.001	143.011	< 0.001	1.017	0.361
APT102 (n = 10)	18.0 ± 4.8	17.1 ± 4.3	11.6 ± 2.6	5.8 ± 1.5						
Edema size (%)										
Control (n = 10)	30.2 ± 4.4	30.8 ± 3.9	26.8 ± 3.5	20.0 ± 2.5	19.016	< 0.001	115.878	< 0.001	1.780	0.190
APT102 (n = 10)	24.0 ± 5.0	24.4 ± 6.5	18.2 ± 4.8	11.2 ± 2.9						
IMH size (%)										
Control (n = 10)	3.9 ± 2.0	5.2 ± 2.3	3.7 ± 1.5	2.7 ± 1.1	7.646	0.013	35.742	< 0.001	0.115	0.886
APT102 (n = 10)	2.3 ± 1.3	3.4 ± 1.8	2.1 ± 1.1	0.9 ± 0.6						
MVO size (%)										
Control (n = 10)	3.8 ± 0.8	3.1 ± 0.9	2.3 ± 0.6	1.0 ± 0.3	4.444	0.049	175.394	< 0.001	0.735	0.463
APT102 (n = 10)	3.3 ± 0.8	2.7 ± 0.7	1.7 ± 0.5	0.6 ± 0.3						
LVMV (mm ³)										
Control (n = 10)	8.8 ± 1.0	8.8 ± 1.0	8.5 ± 1.0	8.2 ± 1.0	0.122	0.731	22.642	< 0.001	0.695	0.487
APT102 (n = 10)	8.6 ± 0.8	8.6 ± 1.0	8.4 ± 0.9	8.1 ± 0.8						

IMH = intramyocardial hemorrhage, LV = left ventricular, LVMV = left ventricular myocardial volume, MVO = microvascular obstruction

APT102 Reduced Myocardial Edema Size

The edema size was significantly smaller in the APT102 group than in the control group ($F = 19.016$, $p < 0.001$) (Table 1). There were significant main effects at all time points ($F = 115.878$, $p < 0.001$) (Table 1), but no significant interactions between groups and time points ($F = 1.780$, $p = 0.190$) (Table 1). The extent of edema at 24 hours and 48 hours was significantly greater than that at 72 hours (both $p < 0.001$) (Fig. 2B) and on day 5 (both $p < 0.001$) (Fig. 2B)

after reperfusion, and there was no significant difference in edema size between 24 hours and 48 hours after reperfusion ($p = 0.277$) (Fig. 2B). When compared with that in the control group, the extent of edema was significantly less in the APT102 group at 24 hours ($24.0 \pm 5.0\%$ vs. $30.2 \pm 4.4\%$, respectively, $p = 0.007$), 48 hours ($24.4 \pm 6.5\%$ vs. $30.8 \pm 3.9\%$, respectively, $p = 0.016$), 72 hours ($18.2 \pm 4.8\%$ vs. $26.8 \pm 3.5\%$, respectively, $p < 0.001$), and on day 5 ($11.2 \pm 2.9\%$ vs. $20.0 \pm 2.5\%$, respectively, $p < 0.001$) after

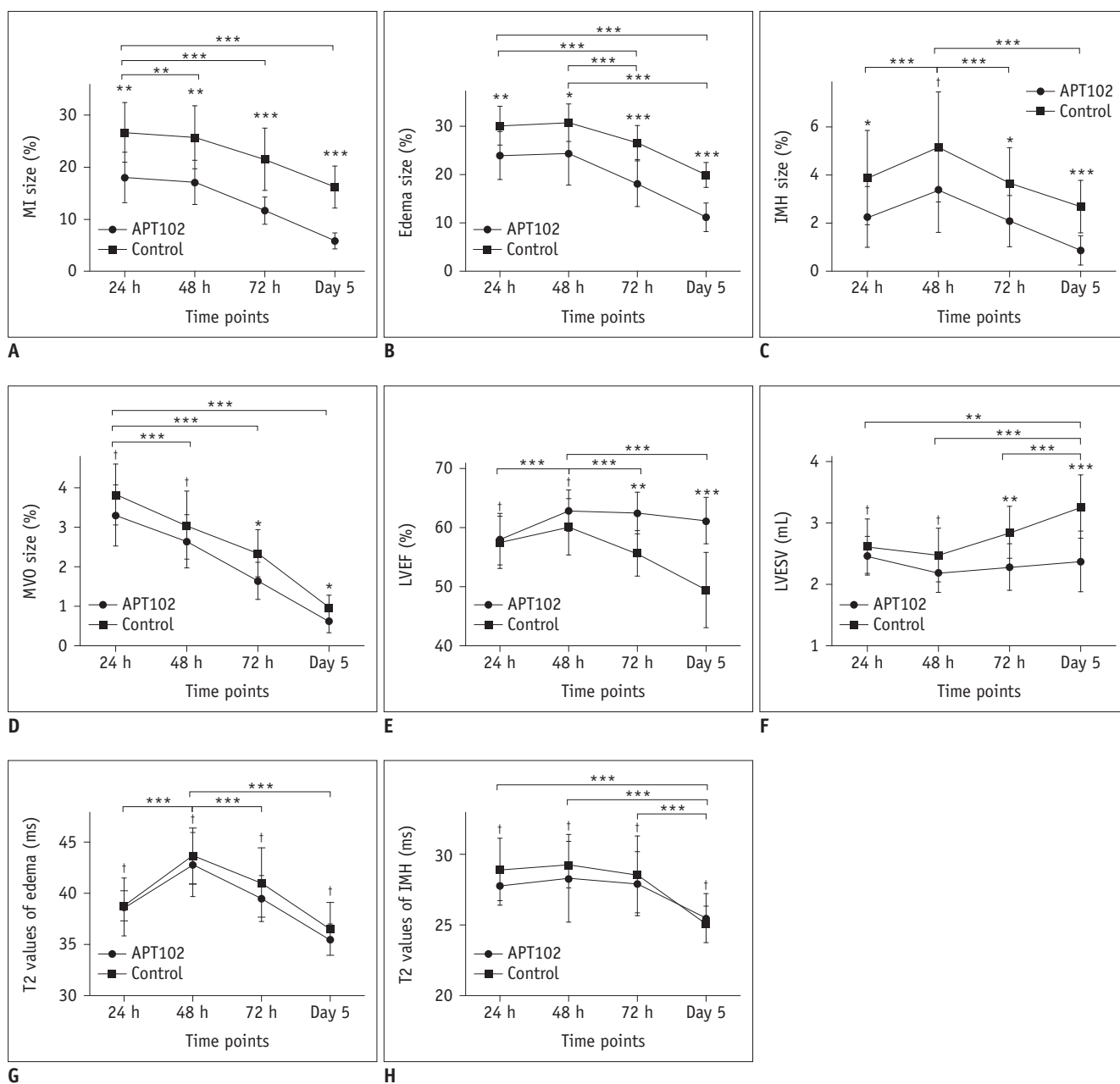


Fig. 2. Temporal evolution of myocardial characterization and left ventricular function in control and APT102 groups. * $p < 0.05$, ** $p < 0.01$, *** $p < 0.001$, † $p > 0.05$. IMH = intramyocardial hemorrhage, LVEF = left ventricular ejection fraction, LVESV = left ventricular end-systolic volume, MI = myocardial infarction, MVO = microvascular obstruction

reperfusion, as shown in Figure 2B.

APT102 Reduced IMH Size

The extent of IMH was significantly less in the APT102 group than in the control group ($F = 7.646$, $p = 0.013$) (Table 1). There were significant main effects at all time points ($F = 35.742$, $p < 0.001$) (Table 1), but no significant interactions between groups and time points ($F = 0.115$, $p = 0.886$) (Table 1). IMH size at 48 hours was significantly greater than at 24 hours, 72 hours, and on day 5 (all $p < 0.001$) (Table 1, Fig. 2C) after reperfusion, which confirmed that the extent of IMH peaked at 48 hours after reperfusion. Additionally, the extent of IMH was significantly less in the APT102 group than in the control group at 24 hours ($2.3 \pm 1.3\%$ vs. $3.9 \pm 2.0\%$, respectively, $p = 0.040$), 72 hours ($2.1 \pm 1.1\%$ vs. $3.7 \pm 1.5\%$, respectively, $p = 0.014$), and on day 5 ($0.9 \pm 0.6\%$ vs. $2.7 \pm 1.1\%$, respectively, $p < 0.001$)

after reperfusion, while there was no significant difference at 48 hours ($3.4 \pm 1.8\%$ vs. $5.2 \pm 2.3\%$, $p = 0.068$) after reperfusion, as shown in Figure 2C. Figure 3 shows CMR images from one APT102 rat and one control rat at four time points after reperfusion showing the extent of IMH and MVO, and the persistently elevated T2 in the surrounding myocardium within the infarct zone.

APT102 Reduced MVO Size

There were significant differences in MVO size between the APT102 and control groups ($F = 4.444$, $p = 0.049$) (Table 1). The extent of MVO was significantly greater at 24 hours after reperfusion than at 48 hours, 72 hours, and on day 5 (all $p < 0.001$) (Table 1, Fig. 2D). The extent of MVO was significantly less in the APT102 group than in the control group at 72 hours ($1.7 \pm 0.5\%$ vs. $2.3 \pm 0.6\%$, respectively, $p = 0.038$) and on day 5 ($0.6 \pm 0.3\%$ vs. 1.0

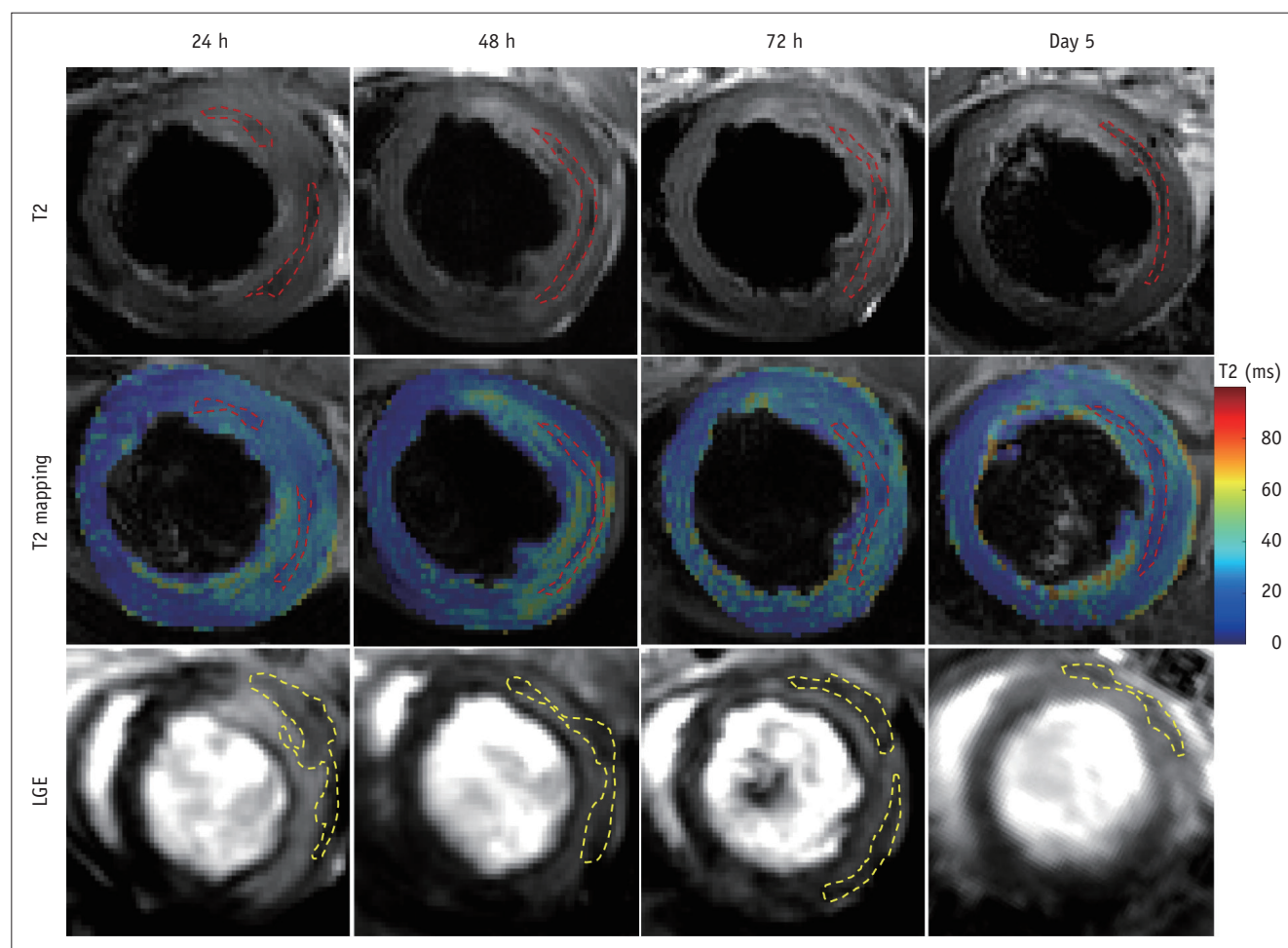


Fig. 3. Sequential changes in CMR images from one control subject (A) and one APT102 subject (B). Red dotted lines show areas of IMH on T2 maps and yellow dotted lines show areas of MVO on LGE images. LGE = late gadolinium enhancement

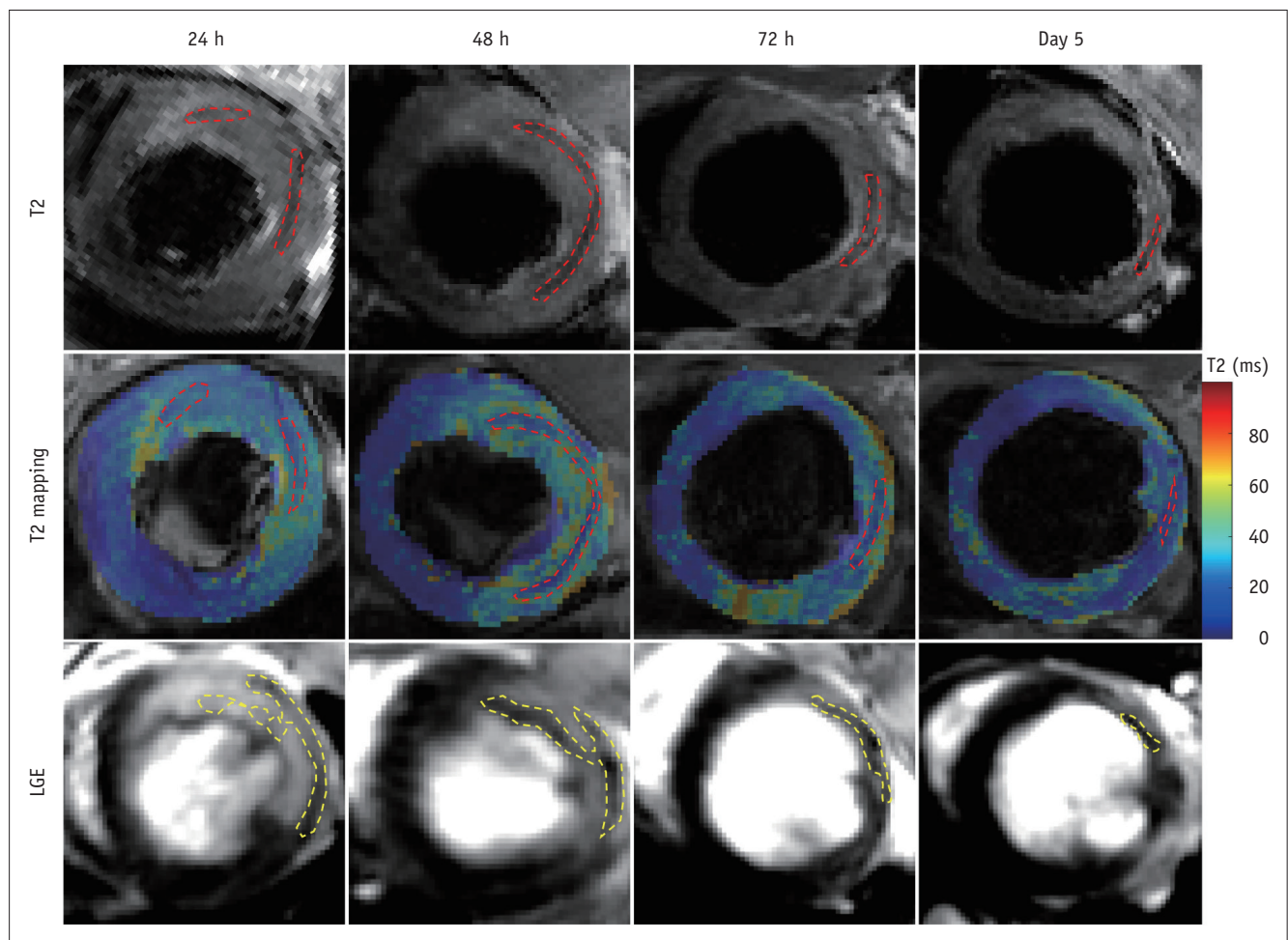


Fig. 3. Sequential changes in CMR images from one control subject (A) and one APT102 subject (B). Red dotted lines show areas of IMH on T2 maps and yellow dotted lines show areas of MVO on LGE images. LGE = late gadolinium enhancement

$\pm 0.3\%$, respectively, $p = 0.021$) after reperfusion, whereas there was no significant difference at 24 hours ($3.3 \pm 0.8\%$ vs. $3.8 \pm 0.8\%$, respectively, $p = 0.146$) or 48 hours ($2.7 \pm 0.7\%$ vs. $3.1 \pm 0.9\%$, respectively, $p = 0.256$) after reperfusion, as shown in Figure 2D.

APT102 Enhanced LV Systolic Function

LVEF was significantly greater in the APT102 group than in the control group ($F = 9.708$, $p = 0.006$) (Table 2). LVEF at 48 hours after reperfusion was significantly greater than at 24 hours, 72 hours, and on day 5, which demonstrates that LVEF peaked at 48 hours after reperfusion, as shown in Figure 2E. LVESV was significantly lower in the APT102 than in the control group ($F = 7.046$, $p = 0.016$) (Table 2). Moreover, there was no significant difference in LVEDV ($F = 1.058$, $p = 0.317$) (Table 2) or SV ($F = 0.335$, $p = 0.570$) (Table 2) between the two groups. The representative cine

images from 24 hours and on day 5 after reperfusion from both groups are shown in Supplementary Movie 1.

Temporal Evolution of T2 Values of Myocardial Edema, IMH, and Remote Zones

There were no significance differences in the T2 values of the remote myocardium, myocardial edema, or IMH between the APT102 and control groups. However, the T2 value of the myocardial edema at 48 hours was significantly greater than at 24 hours, 72 hours, and on day 5 after reperfusion. The T2 value of IMH on day 5 after reperfusion was significantly lower than at 24 hours, 48 hours, and 72 hours after reperfusion (Table 3, Fig. 2G, H).

Relationship between MI, IMH, MVO, and LVEF

Intra- and interobserver reliability of the measurement of the infarct, edema IMH, and MVO area is shown in Table 4.

Table 2. Comparison of LV Systolic Function according to Time Points and Groups

Variable	24 h	48 h	72 h	Day 5	Group		Time		Group x Time		
					F	P	F	P	F	P	
LVEDV (mL)											
Control (n = 10)	6.2 ± 0.6	6.2 ± 0.6	6.4 ± 0.7	6.6 ± 0.8	1.058	0.317	10.439	< 0.001	2.008	0.147	
APT102 (n = 10)	5.9 ± 0.8	5.9 ± 0.8	6.1 ± 0.8	6.1 ± 1.0							
LVESV (mL)											
Control (n = 10)	2.6 ± 0.5	2.5 ± 0.4	2.9 ± 0.4	3.3 ± 0.5	7.046	0.016	31.465	< 0.001	21.065	< 0.001	
APT102 (n = 10)	2.5 ± 0.3	2.2 ± 0.3	2.3 ± 0.4	2.4 ± 0.5							
SV (mL)											
Control (n = 10)	3.5 ± 0.4	3.7 ± 0.4	3.6 ± 0.4	3.3 ± 0.6	0.335	0.570	6.912	0.003	5.372	0.009	
APT102 (n = 10)	3.5 ± 0.7	3.7 ± 0.6	3.8 ± 0.5	3.7 ± 0.6							
LVEF (%)											
Control (n = 10)	57.5 ± 4.4	60.2 ± 4.8	55.7 ± 3.8	49.5 ± 6.4	9.708	0.006	23.765	< 0.001	21.202	< 0.001	
APT102 (n = 10)	58.1 ± 4.4	62.9 ± 3.5	62.5 ± 3.5	61.2 ± 3.9							

LVEDV = left ventricular end-diastolic volume, LVEF = left ventricular ejection fraction, LVESV = left ventricular end-systolic volume, SV = stroke volume

Table 3. Comparison of T2 Value according to Time Points and Groups

Variable	24 h	48 h	72 h	Day 5	Group		Time		Group x Time		
					F	P	F	P	F	P	
Remote T2 values (ms)											
Control (n = 10)	22.4 ± 0.6	22.3 ± 0.4	22.5 ± 0.4	22.3 ± 0.5	2.206	0.155	0.056	0.982	0.351	0.784	
APT102 (n = 10)	22.1 ± 0.5	22.2 ± 0.6	22.1 ± 0.4	22.2 ± 0.7							
Edema T2 values (ms)											
Control (n = 10)	38.8 ± 1.5	43.7 ± 2.7	41.1 ± 3.4	36.5 ± 2.6	1.320	0.266	37.400	< 0.001	0.462	0.620	
APT102 (n = 10)	38.7 ± 2.8	42.8 ± 3.1	39.5 ± 2.3	35.5 ± 1.5							
IMH T2 values (ms)											
Control (n = 10)	28.9 ± 2.2	29.3 ± 1.7	28.6 ± 2.7	25.1 ± 1.3	0.713	0.410	23.055	< 0.001	0.462	0.710	
APT102 (n = 10)	27.8 ± 1.4	28.3 ± 3.1	28.0 ± 2.3	25.5 ± 1.7							

Table 4. Intra- and Interobserver Reliability of Measurement of Infarct, Edema, IMH and MVO Size, Described with ICCs and 95% CIs

Measurement	ICC (95% CI)	
	Intraobserver	Interobserver
Infarct size	0.973 (0.956–0.983)	0.942 (0.906–0.964)
Edema size	0.963 (0.932–0.978)	0.855 (0.761–0.911)
IMH size	0.987 (0.980–0.992)	0.943 (0.912–0.963)
MVO size	0.980 (0.969–0.987)	0.927 (0.888–0.952)

CI = confidence interval, ICC = intraclass correlation coefficient

There was a significant and negative correlation between LVEF and MI size ($r = -0.230$, $p = 0.046$), and IMH size ($r = -0.294$, $p = 0.010$), and a significant and positive correlation between IMH size and MVO size ($r = 0.392$, $p < 0.001$), while no significant correlation was found between LVEF and edema size ($r = 0.184$, $p = 0.112$), and MVO size ($r = 0.065$, $p = 0.574$), as shown in Figure 4.

Histopathological Findings

Bland-Altman plots showed that the volume of IMH measured on T2 mapping images matched well with the gross pathology images (Fig. 5). Figure 6 shows the CMR images and corresponding slices of the gross pathologic images, as well as H&E-stained images of the heart sections from representative subjects. The distinct red to reddish black areas on gross sections were defined as areas of IMH, where red blood cells and inflammatory cells caused swelling of the myocardial interstitium.

DISCUSSION

It is well known that there is a strong association between the extent of MVO and IMH with a reported correlation coefficient of IMH of 0.80–0.87 for late MVO (21, 22). Likewise, there was also a positive correlation in the present study ($r = 0.392$). We observed that the extent

of MVO peaked at 24 hours after reperfusion and decreased thereafter, while IMH size peaked at 48 hours after reperfusion and then decreased thereafter. The observed

temporal evolution of IMH and MVO was consistent with the clinical study by Carrick et al. (23), where MVO peaked at 4 to 12 hours post reperfusion, whereas IMH increased

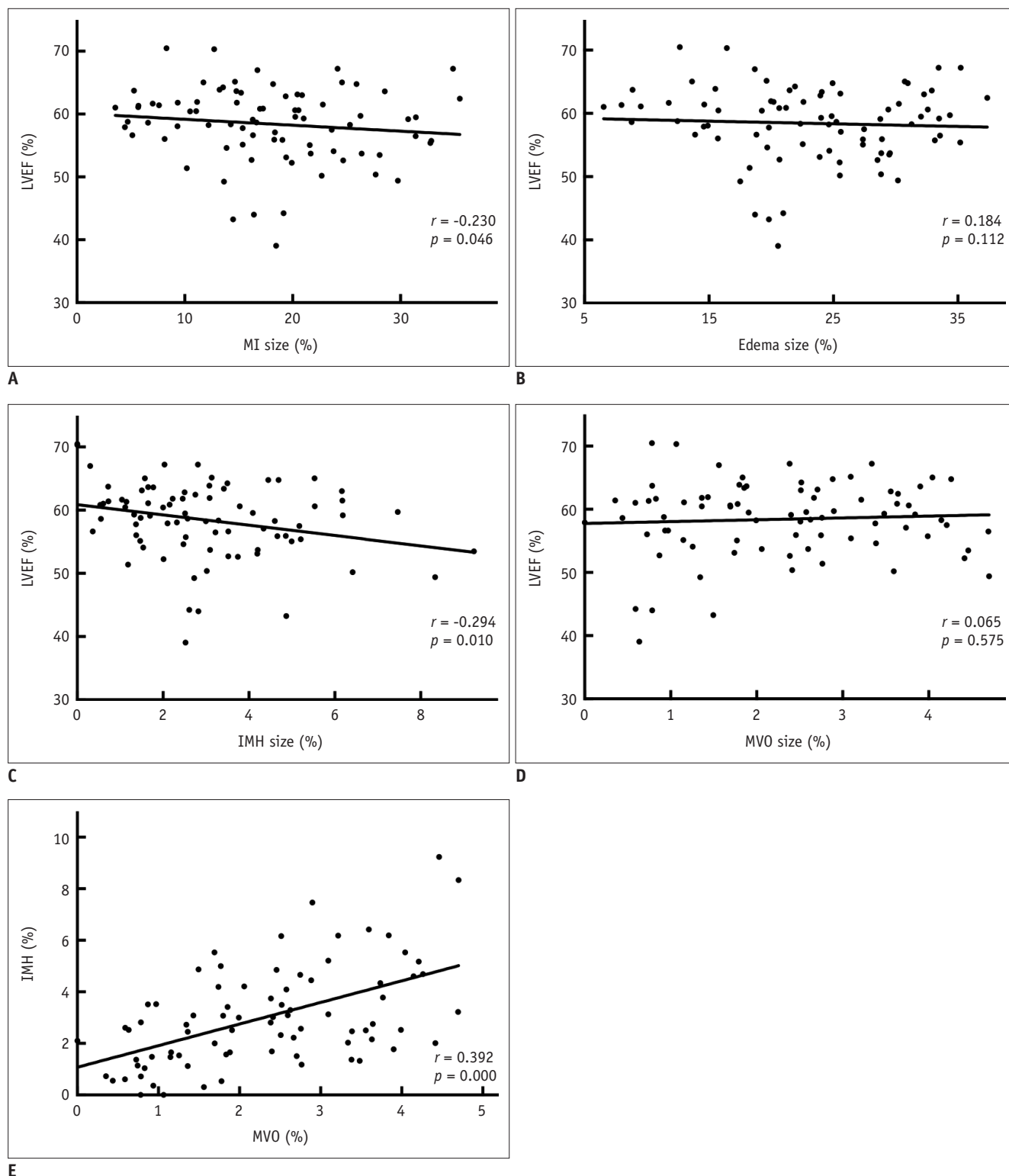


Fig. 4. Linear correlation between extent of MI, IMH, MVO, and LVEF. There was negative correlation between LVEF and MI size (A), and IMH size (C), and positive correlation between IMH size and MVO size (E), while no significant correlation was found between LVEF and edema size (B), and MVO size (D).

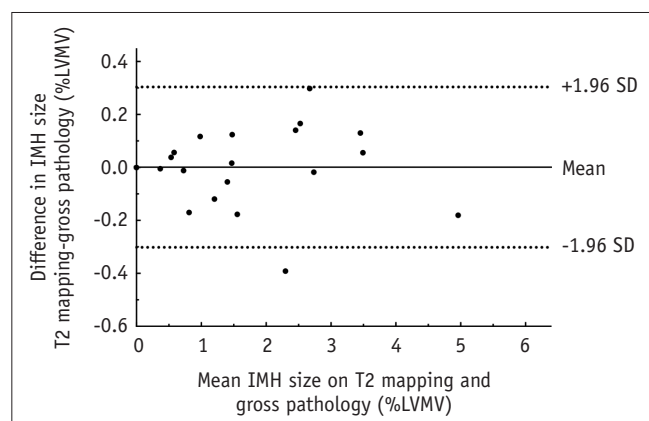
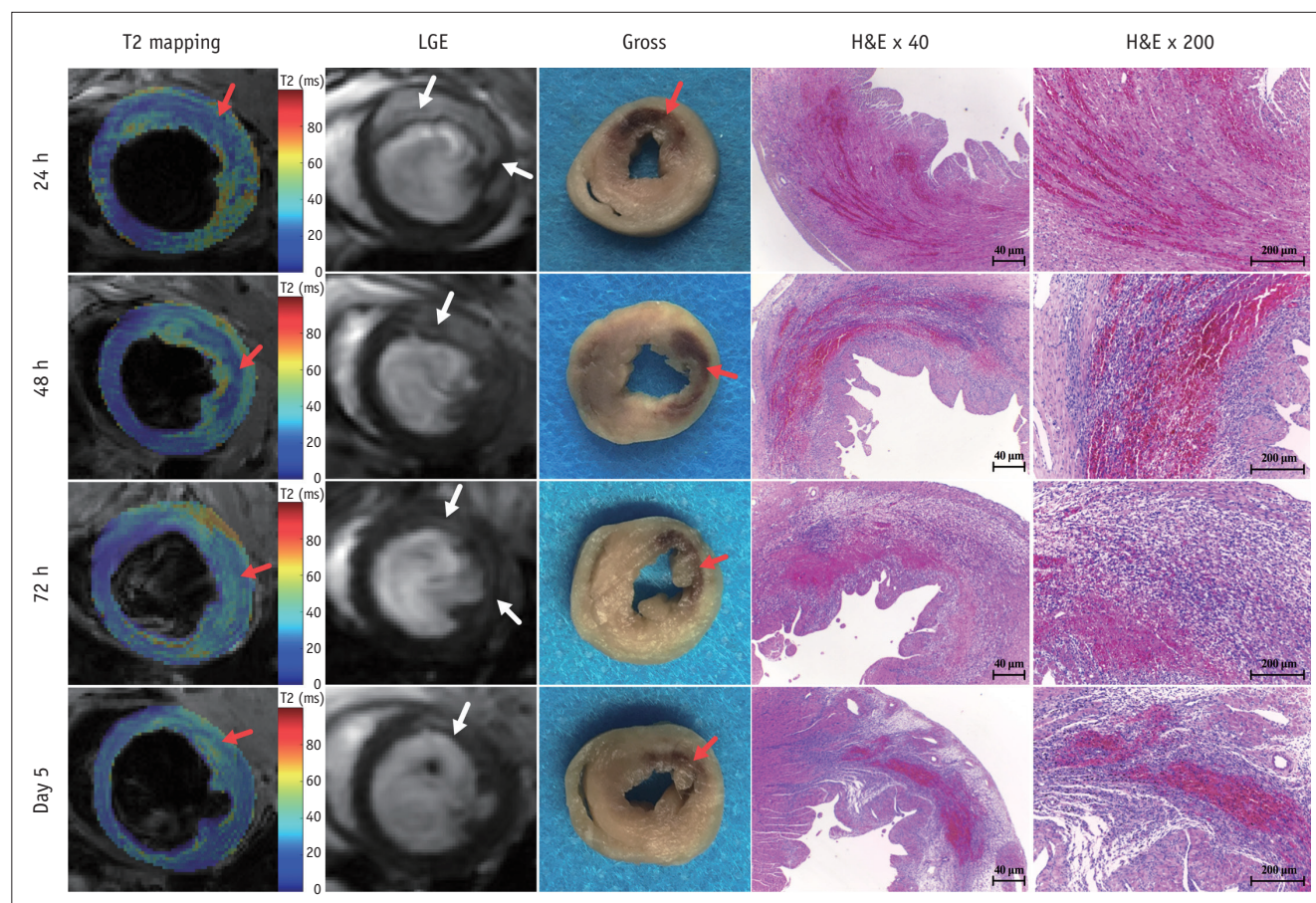
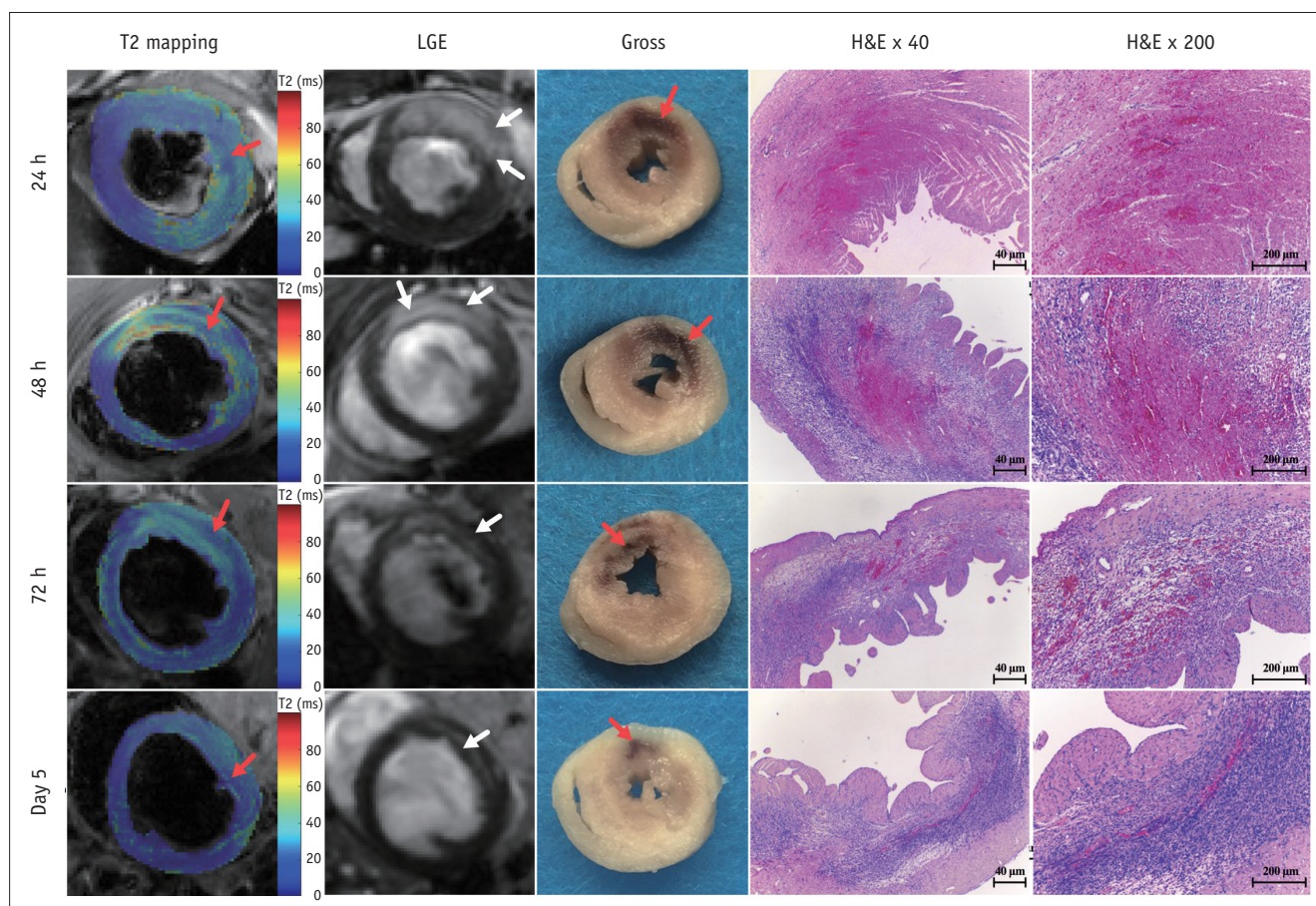


Fig. 5. Comparison of IMH size on day 5 after reperfusion as measured using T2 mapping with pathological gross examination. Bland-Altman plot shows that IMH size measured using T2 mapping and pathological gross examination were not significantly different (mean difference 0.0008%, 95% limit of agreement from -0.3019% to 0.3036%). LVMV = left ventricular myocardial volume, SD = standard deviation

progressively and peaked at 72 hours post reperfusion. The results of that study and the present study indicated that MVO almost precedes IMH in the temporal evolution of IRI and IMH is the downstream consequence of MVO. Furthermore, the extent of IMH was approximately equal to or greater than that of MVO at different time points, and regions of late MVO almost coincided with regions of IMH. Because of the slow diffusion of Gd-DTPA over time around the periphery of no-flow regions, the extent of MVO seen on LGE may be smaller than that on either first pass perfusion or early gadolinium enhancement (24). Furthermore, FISP-cine with a relatively long acquisition time in the present study may have also contributed to the underestimation of the extent of MVO (16). Previous studies using canine and porcine models with 90-minute occlusion of the left anterior descending branch have demonstrated an almost 3-fold increase in MVO size over the first 48 hours post reperfusion (25), while our data showed that MVO peaked



A
Fig. 6. CMR images and corresponding pathology at four time points after reperfusion of control subjects (A) and APT102 subjects (B). Red arrows show areas of IMH on T2 maps and gross sections and white arrows show areas of MVO on LGE images. H&E = hematoxylin and eosin



B

Fig. 6. CMR images and corresponding pathology at four time points after reperfusion of control subjects (A) and APT102 subjects (B). Red arrows show areas of IMH on T2 maps and gross sections and white arrows show areas of MVO on LGE images. H&E = hematoxylin and eosin

at 24 hours post reperfusion, which may be ascribed to the different occlusion times of the left anterior descending branch and differences in animal models.

A great number of studies (23, 26-28) have provided strong evidence that IMH and residual myocardial iron are adverse prognostic complications in reperfused STEMI patients and porcine models. In this study, a negative correlation was also demonstrated between IMH and LVEF ($r = -0.294$). Thus, IMH may be a potential therapeutic target for the prevention of adverse LV remodeling and the occurrence time of IMH suggests a therapeutic window may exist to efficiently prevent IMH. Human E-NTPDase-1/CD39 is an extracellular nucleotide that hydrolyzes extracellular ATP and ADP to AMP, which is converted to adenosine by CD73 (11, 29). In addition, CD39 can impede ATP and ADP interactions at platelet P2 receptors (11). Thus, CD39 could efficiently inhibit inflammation and thrombosis while maintaining vascular integrity. Köhler et al. (15) suggested

that ischemic preconditioning with brief cycles of short-term coronary occlusion and reperfusion performed before prolonged coronary artery occlusion with reperfusion could increase the expression of CD39 by the endothelia and myocytes and reduce infarct size, while this work did not report a powerful effect on IMH and MVO (15). In the present study, APT102 not only reduced the extent of infarction and edema, but also the extent of IMH and MVO, which has not been reported before.

In the present study, the mean T2 values of myocardial edema at 24 hours and 48 hours after reperfusion were 38.8 ± 1.5 ms and 43.7 ± 2.7 ms in the control group, which were close to the values of 34.7 ± 6.7 ms and 47.7 ± 6.6 ms acquired in previous studies (16, 30, 31). The mean T2 value of IMH at 48 hours (29.3 ± 1.7 ms) was also similar to that in a previous study (27.6 ± 3.3 ms) (16), where T2 values of remote myocardium were greater (22.3 ± 0.4 ms) but lower than those of edema (43.7 ± 2.7 ms), reflecting

the contrasting effects of hemorrhage, which tends to shorten T2, with that of edema, which increases T2 (16, 32).

Lastly, there was an apparent discrepancy between the delayed recovery of LV systolic function and the maximal extent of IMH and edema at 48 hours post reperfusion in the APT102 and control groups. Our data disclosed that LVEF at 48 hours was greater than that at 24 hours, while LVESV was lower than that at 24 hours. This phenomenon can be explained by the delay in functional recovery of the salvaged myocardium, where stunning can occur. Myocardial stunning is a reversible injury where postischemic myocardial function can recover to preischemic levels upon reperfusion (33).

Supplementary Materials

The Data Supplement is available with this article at <https://doi.org/10.3348/kjr.2019.0853>.

Supplementary Movie Legends

Movie 1. Representative cine images from 24 hours and on day 5 after reperfusion from control subjects (A) and APT102 subjects (B).

The infarcted wall of the control subject is thinner than the APT102 subject, and the wall contraction of the control subject is weaker than the APT102 subject.

Conflicts of Interest

The authors have no potential conflicts of interest to disclose.

ORCID iDs

Fabao Gao

<https://orcid.org/0000-0003-2257-3275>

Ziqian Xu

<https://orcid.org/0000-0002-5142-7704>

Wei Chen

<https://orcid.org/0000-0003-2551-4916>

Ruzhi Zhang

<https://orcid.org/0000-0001-8292-0270>

Lei Wang

<https://orcid.org/0000-0001-9695-3196>

Ridong Chen

<https://orcid.org/0000-0001-9323-2000>

Jie Zheng

<https://orcid.org/0000-0002-4033-2718>

REFERENCES

1. Keeley EC, Boura JA, Grines CL. Comparison of primary and facilitated percutaneous coronary interventions for ST-elevation myocardial infarction: quantitative review of randomised trials. *Lancet* 2006;367:579-588
2. Yellon DM, Hausenloy DJ. Myocardial reperfusion injury. *N Engl J Med* 2007;357:1121-1135
3. Hearse DJ, Tosaki A. Free radicals and reperfusion-induced arrhythmias: protection by spin trap agent PBN in the rat heart. *Circ Res* 1987;60:375-383
4. Kloner RA, Bolli R, Marban E, Reinlib L, Braunwald E. Medical and cellular implications of stunning, hibernation, and preconditioning: an NHLBI workshop. *Circulation* 1998;97:1848-1867
5. Wu KC, Zerhouni EA, Judd RM, Lugo-Olivieri CH, Barouch LA, Schulman SP, et al. Prognostic significance of microvascular obstruction by magnetic resonance imaging in patients with acute myocardial infarction. *Circulation* 1998;97:765-772
6. Ochiai K, Shimada T, Murakami Y, Ishibashi Y, Sano K, Kitamura J, et al. Hemorrhagic myocardial infarction after coronary reperfusion detected in vivo by magnetic resonance imaging in humans: prevalence and clinical implications. *J Cardiovasc Magn Reson* 1999;1:247-256
7. Piper HM, García-Dorado D, Ovize M. A fresh look at reperfusion injury. *Cardiovasc Res* 1998;38:291-300
8. Hamirani YS, Wong A, Kramer CM, Salerno M. Effect of microvascular obstruction and intramyocardial hemorrhage by CMR on LV remodeling and outcomes after myocardial infarction: a systematic review and meta-analysis. *JACC Cardiovasc Imaging* 2014;7:940-952
9. Cauwels A, Rogge E, Vandendriessche B, Shiva S, Brouckaert P. Extracellular ATP drives systemic inflammation, tissue damage and mortality. *Cell Death Dis* 2014;5:e1102
10. Smith SB, Xu Z, Novitskaya T, Zhang B, Chepurko E, Pu XA, et al. Impact of cardiac-specific expression of CD39 on myocardial infarct size in mice. *Life Sci* 2017;179:54-59
11. Moeckel D, Jeong SS, Sun X, Broekman MJ, Nguyen A, Drosopoulos JHF, et al. Optimizing human apyrase to treat arterial thrombosis and limit reperfusion injury without increasing bleeding risk. *Sci Transl Med* 2014;6:248ra105
12. Tan Z, Li X, Turner RC, Logsdon AF, Lucke-Wold B, DiPasquale K, et al. Combination treatment of r-tPA and an optimized human apyrase reduces mortality rate and hemorrhagic transformation 6h after ischemic stroke in aged female rats. *Eur J Pharmacol* 2014;738:368-373
13. Ibrahim M, Wang X, Puyo CA, Montecalvo A, Huang HJ, Hachem RR, et al. Human recombinant apyrase therapy protects against canine pulmonary ischemia-reperfusion injury. *J Heart Lung Transplant* 2015;34:247-253
14. Sugimoto S, Lin X, Lai J, Okazaki M, Das NA, Li W, et al. Apyrase treatment prevents ischemia-reperfusion injury in rat lung isografts. *J Thorac Cardiovasc Surg* 2009;138:752-759
15. Köhler D, Eckle T, Faigle M, Grenz A, Mittelbronn M, Laucher S,

- et al. CD39/ectonucleoside triphosphate diphosphohydrolase 1 provides myocardial protection during cardiac ischemia/reperfusion injury. *Circulation* 2007;116:1784-1794
16. Chen W, Zhang B, Xia R, Zhang R, Xu Z, Chen Y, et al. T2 mapping at 7T MRI can quantitatively assess intramyocardial hemorrhage in rats with acute reperfused myocardial infarction in vivo. *J Magn Reson Imaging* 2016;44:194-203
17. Ugander M, Bagi PS, Oki AJ, Chen B, Hsu LY, Aletras AH, et al. Myocardial edema as detected by pre-contrast T1 and T2 CMR delineates area at risk associated with acute myocardial infarction. *JACC Cardiovasc Imaging* 2012;5:596-603
18. Kali A, Tang RL, Kumar A, Min JK, Dharmakumar R. Detection of acute reperfusion myocardial hemorrhage with cardiac MR imaging: T2 versus T2. *Radiology* 2013;269:387-395
19. Bondarenko O, Beek AM, Hofman MB, Kühl HP, Twisk JW, van Dockum WG, et al. Standardizing the definition of hyperenhancement in the quantitative assessment of infarct size and myocardial viability using delayed contrast-enhanced CMR. *J Cardiovasc Magn Reson* 2005;7:481-485
20. Robbers LF, Eerenberg ES, Teunissen PF, Jansen MF, Hollander MR, Horrevoets AJ, et al. Magnetic resonance imaging-defined areas of microvascular obstruction after acute myocardial infarction represent microvascular destruction and haemorrhage. *Eur Heart J* 2013;34:2346-2353
21. Bekkers SC, Smulders MW, Passos VL, Leiner T, Waltenberger J, Gorgels AP, et al. Clinical implications of microvascular obstruction and intramyocardial haemorrhage in acute myocardial infarction using cardiovascular magnetic resonance imaging. *Eur Radiol* 2010;20:2572-2578
22. Beek AM, Nijveldt R, van Rossum AC. Intramyocardial hemorrhage and microvascular obstruction after primary percutaneous coronary intervention. *Int J Cardiovasc Imaging* 2010;26:49-55
23. Carrick D, Haig C, Ahmed N, McEntegart M, Petrie MC, Eteiba H, et al. Myocardial hemorrhage after acute reperfused ST-segment-elevation myocardial infarction: relation to microvascular obstruction and prognostic significance. *Circ Cardiovasc Imaging* 2016;9:e004148
24. Mather AN, Lockie T, Nagel E, Marber M, Perera D, Redwood S, et al. Appearance of microvascular obstruction on high resolution first-pass perfusion, early and late gadolinium enhancement CMR in patients with acute myocardial infarction. *J Cardiovasc Magn Reson* 2009;11:33
25. Ghugre NR, Ramanan V, Pop M, Yang Y, Barry J, Qiang B, et al. Quantitative tracking of edema, hemorrhage, and microvascular obstruction in subacute myocardial infarction in a porcine model by MRI. *Magn Reson Med* 2011;66:1129-1141
26. Kali A, Kumar A, Cokic I, Tang RLQ, Tsaftaris SA, Friedrich MG, et al. Chronic manifestation of postreperfusion intramyocardial hemorrhage as regional iron deposition: a cardiovascular magnetic resonance study with ex vivo validation. *Circ Cardiovasc Imaging* 2013;6:218-228
27. Bulluck H, Rosmini S, Abdel-Gadir A, White SK, Bhuva AN, Treibel TA, et al. Residual myocardial iron following intramyocardial hemorrhage during the convalescent phase of reperfused ST-segment-elevation myocardial infarction and adverse left ventricular remodeling. *Circ Cardiovasc Imaging* 2016;9:e004940
28. Ghugre NR, Pop M, Thomas R, Newbigging S, Qi X, Barry J, et al. Hemorrhage promotes inflammation and myocardial damage following acute myocardial infarction: insights from a novel preclinical model and cardiovascular magnetic resonance. *J Cardiovasc Magn Reson* 2017;19:50
29. Antonioli L, Pacher P, Vizi ES, Haskó G. CD39 and CD73 in immunity and inflammation. *Trends Mol Med* 2013;19:355-367
30. Xia R, Lu X, Zhang B, Wang Y, Liao J, Zheng J, et al. Assessment of myocardial edema and area at risk in a rat model of myocardial infarction with a faster T2 mapping method. *Acta Radiol* 2015;56:1085-1090
31. Xia R, Lu X, Zhang B, Wang Y, Liao J, Zheng J, et al. Early reperfusion can reduce infarction size but not salvaged myocardial size in acute myocardial infarction rats. *JACC Cardiovasc Imaging* 2015;8:616-617
32. O'Regan DP, Ahmed R, Karunanithy N, Neuwirth C, Tan Y, Durighel G, et al. Reperfusion hemorrhage following acute myocardial infarction: assessment with T2* mapping and effect on measuring the area at risk. *Radiology* 2009;250:916-922
33. Neri M, Riezzo I, Pascale N, Pomara C, Turillazzi E. Ischemia/reperfusion injury following acute myocardial infarction: a critical issue for clinicians and forensic pathologists. *Mediators Inflamm* 2017;2017:7018393